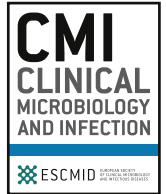




Contents lists available at ScienceDirect

## Clinical Microbiology and Infection

journal homepage: [www.clinicalmicrobiologyandinfection.com](http://www.clinicalmicrobiologyandinfection.com)

## Original article

Quantification of within-patient *Staphylococcus aureus* phenotypic heterogeneity as a proxy for the presence of persisters across clinical presentations

Julian Bär<sup>1,†</sup>, Mathilde Boumassoud<sup>1,†</sup>, Srikanth Mairpady Shambat<sup>1,†</sup>, Clément Vulin<sup>1</sup>, Markus Huemer<sup>1</sup>, Tiziano A. Schweizer<sup>1</sup>, Alejandro Gómez-Mejía<sup>1</sup>, Nadia Eberhard<sup>1</sup>, Yvonne Achermann<sup>1</sup>, Patrick O. Zingg<sup>2</sup>, Carlos A. Mestres<sup>3</sup>, Silvio D. Brugger<sup>1</sup>, Reto A. Schuepbach<sup>4</sup>, Roger D. Kouyos<sup>1</sup>, Barbara Hase<sup>1</sup>, Annelies S. Zinkernagel<sup>1,\*</sup>

<sup>1</sup> Department of Infectious Diseases and Hospital Epidemiology, University Hospital Zurich, University of Zurich, Zurich, Switzerland

<sup>2</sup> Balgrist University Hospital, University of Zurich, Zurich, Switzerland

<sup>3</sup> Clinic for Cardiovascular Surgery, University Hospital Zurich, University of Zurich, Zurich, Switzerland

<sup>4</sup> Institute for Intensive Care Medicine, University Hospital Zurich, University of Zurich, Zurich, Switzerland

## ARTICLE INFO

## Article history:

Received 28 September 2021

Received in revised form

19 January 2022

Accepted 23 January 2022

Available online xxx

Editor: G. Lina

## Keywords:

Antibiotic tolerance

Biofilm

Phenotypic heterogeneity

Rifampicin

*Staphylococcus aureus*

## ABSTRACT

**Objectives:** Difficult-to-treat infections caused by antibiotic-susceptible strains have been linked to the occurrence of persisters, a subpopulation of dormant bacteria that tolerate antibiotic exposure despite lacking genetic resistance. These persisters can be identified phenotypically by plating on nutrient agar because of their altered growth dynamics, resulting in colony-size heterogeneity. The occurrence of within-patient bacterial phenotypic heterogeneity in various infections and clinical determinants of persister formation remains unknown.

**Methods:** We plated bacteria derived from 132 patient samples of difficult-to-treat infections directly on nutrient-rich agar and monitored colony growth by time-lapse imaging. We retained 36 *Staphylococcus aureus* monocultures for further analysis. We investigated clinical factors associated with increased colony growth-delay with regression analyses. We corroborated the clinical findings using *in vitro* grown static biofilms exposed to distinct antibiotics.

**Results:** The extent of phenotypic heterogeneity of patient-derived *S. aureus* varied substantially between patients (from no delay to a maximum of 57.6 hours). Increased heterogeneity coincided with increased median colony growth-delay. Multivariable regression showed that rifampicin treatment was significantly associated with increased median growth-delay (13.3 hours; 95% CI 7.13–19.6 hours;  $p < 0.001$ ). *S. aureus* grown in biofilms and exposed to high concentrations of rifampicin or a combination of rifampicin with clindamycin or levofloxacin exhibited prolonged growth-delay ( $p < 0.05$  for 11 of 12 comparisons), correlating with a strain-dependent increase in antibiotic tolerance.

**Discussion:** Colony-size heterogeneity upon direct sampling of difficult-to-treat *S. aureus* infections was frequently observed. Hence, future studies are needed to assess the potential benefit of phenotypic heterogeneity quantification for staphylococcal infection prognosis and treatment guidelines. **Julian Bär, Clin Microbiol Infect 2022;■:1**

© 2022 The Authors. Published by Elsevier Ltd on behalf of European Society of Clinical Microbiology and Infectious Diseases. This is an open access article under the CC BY-NC-ND license (<http://creativecommons.org/licenses/by-nc-nd/4.0/>).

## Introduction

*Staphylococcus aureus* is frequently part of the normal flora and a cause of infection in humans [1]. Deep-seated infections, such as cardiovascular infections (CVIs) and prosthetic joint infections (PJIs), are usually difficult to treat due to the presence of biofilms

\* Corresponding author. Annelies Zinkernagel, Rämistrasse 100, 8091 Zürich, Switzerland.

E-mail address: [annelies.zinkernagel@usz.ch](mailto:annelies.zinkernagel@usz.ch) (A.S. Zinkernagel).

† Julian Bär, Mathilde Boumassoud, and Srikanth Mairpady Shambat contributed equally to this work.

<https://doi.org/10.1016/j.cmi.2022.01.021>

1198-743X/© 2022 The Authors. Published by Elsevier Ltd on behalf of European Society of Clinical Microbiology and Infectious Diseases. This is an open access article under the CC BY-NC-ND license (<http://creativecommons.org/licenses/by-nc-nd/4.0/>).

Please cite this article as: Bär J et al., Quantification of within-patient *Staphylococcus aureus* phenotypic heterogeneity as a proxy for the presence of persisters across clinical presentations, *Clinical Microbiology and Infection*, <https://doi.org/10.1016/j.cmi.2022.01.021>

[2]. They often require prolonged antibiotic treatment, surgical debridement, and removal of prosthetic material.

Prolonged antibiotic treatment facilitates the emergence of antibiotic resistance [3], which can be preceded by antibiotic tolerance [4,5], defined as the ability of an antibiotic-susceptible bacterial population to survive a time-limited antibiotic challenge [6,7]. This property can be conferred by mutations affecting growth rate or by phenotypic switching to a dormant state [8]. The resulting slow- or non-growing bacteria, termed persisters, have been implicated in difficult-to-treat and relapsing *S. aureus* infections [9–12].

A subpopulation of persisters can be identified by plating on nutrient-rich agar owing to their altered growth dynamics. In the case of mutations affecting growth rate, stable small colony variants can be observed [13,14]. Yet most often, *S. aureus* isolated from infection sites has been reported to give rise to nonstable small colonies, which result from heterogeneous delays in the growth resumption of bacterial cells. This heterogeneity in dormancy can be induced by exposure to stressors, such as low pH, antibiotic exposure, biofilm, or intracellular environment [10,15–17], and reverts when the stress is removed. An infecting strain is likely to encounter most of these stressors within a patient, but frequency and clinical determinants of within-patient bacterial phenotypic heterogeneity are currently unknown. Few studies have monitored the colony growth of bacterial populations directly after recovery from human infection sites and usually included a small number of patients [12,15,18].

Here, we provide the first descriptive epidemiologic study quantifying the occurrence of within-patient *S. aureus* phenotypic heterogeneity as a proxy for the presence of persisters in distinct clinical presentations.

## Methods

### Ethics

Approval was given by the ethics committee of the Canton of Zurich, Switzerland (Kantonale Ethikkommission Zurich) for the Vascular Graft Cohort study (VASGRA; KEK-2012-0583), Endovascular and Cardiac Valve Infection Registry (ENVALVE; BASEC 2017-01140), Prosthetic Joint Infection Cohort (Balgrist, BASEC 2017-01458), and BacVivo (BASEC 2017-02225). Patient consent was obtained from all participants within the framework of these studies.

### Sample collection and processing

This study took place between October 2016 and May 2020 at two tertiary care hospitals in Switzerland: University Hospital of Zurich and Balgrist University Hospital. During this timeframe, we applied a convenience sampling strategy to acquire material from medical procedures performed in patients with suspected staphylococcal infections (Method S1). For five participants, more than one sample was obtained (Method S2).

Patient-derived material was homogenized, eukaryotic cells were lysed, and antibiotics were washed out (Fig. 1A; Method S3). Isolated bacteria were then spread-plated on Columbia sheep blood agar (CSB, BioMérieux, Switzerland). Absence of growth was interpreted based on parallel routine diagnostic tests (Method S3; Fig. 1B).

### Clinical isolates and subculturing

Clinical isolates were stored at  $-80^{\circ}\text{C}$  by pooling all colonies from the plate into a 40% glycerol stock. For further assays, clinical isolates were streaked on CSB plates, and single colonies were

inoculated into tryptic soy broth (TSB) for overnight growth. The antibiotic susceptibility profile of each isolate was assessed (Method S4; Table S1).

### Imaging of bacterial colonies

To monitor the growth of bacterial colonies, CSB plates were incubated at  $37^{\circ}\text{C}$  and imaged automatically every 10 minutes, using a previously described time-lapse setup [19]. In a few cases, single timepoint images (endpoint images) were manually acquired.

### Colony appearance-time and growth-delay definition

Colony appearance-time was derived from images using Col-Tapp (Method S5) [19]. Growth-delay distributions were obtained by subtracting from the appearance-time distributions the baseline appearance-time of the corresponding clinical isolate (median appearance-time of exponential culture; Figs. S1 and S2; Method S5). Usually, plates with 20 to 250 colonies were selected to facilitate analysis and overcome a potential bias resulting from colony density on appearance-time estimation from endpoint images (Method S6; Fig. S3).

### Biofilm assay

*S. aureus* cultures were grown statically at  $37^{\circ}\text{C}$  in TSB supplemented with 0.15% glucose in 96-well microplates (Method S7). After 24 hours, the supernatant was replaced with fresh medium containing  $10\times$  or  $100\times$  minimum inhibitory concentration (MIC) antibiotics or phosphate-buffered saline. After 24 hours, the antibiotics were washed out. Viable bacterial load (colony-forming units/mL) and appearance-time were quantified by spread-plating on CSB agar (Method S7; Figs. S4 and S5). The proportion of rifampicin (RIF)-resistant mutants was assessed using TSB agar containing  $100\times$  MIC RIF. To rule out the possibility that genetic diversity explained the observed heterogeneous phenotypes, whole-genome sequencing was performed on representative colonies from one experiment (Method S8; Fig. S6).

### Antibiotic persister assay

Bacterial populations were diluted to an aimed inoculum of  $2 \times 10^5$  colony-forming units/mL in TSB, supplemented with either  $40\times$  MIC flucloxacillin (FLX) or phosphate-buffered saline, incubated at  $37^{\circ}\text{C}$ , shaking at 220 rpm. Viable bacterial load was monitored over time by subsampling the cultures, washing out antibiotics, and spot-plating serial dilutions.

### Statistical analysis

Statistical analyses were performed using R 4.0.3, R Studio, and ggplot2 [20]. The effect of clinical parameters on the median growth-delay of bacteria isolated from patients was assessed with univariable and multivariable linear regressions. Dunnett tests were used to compare *in vitro* antibiotic treatments with the control. Specific pairwise comparisons were computed from linear regressions with interaction terms, followed by estimated marginal means *post hoc* tests (multivariate *t* distribution-based *p*-value correction) [21].

### Data availability

Detailed methods and additional figures and tables are provided in the Supplementary Material. Images and raw data are available on the Image Dataset Resource repository (<https://idr.openmicroscopy.org>)

under accession number idr0127. Data underlying figures are available on Figshare (<https://doi.org/10.6084/m9.figshare.15010941>). Sequencing data are available through the European Nucleotide Archive (project PRJEB48885) (<https://www.ebi.ac.uk/ena/browser/view/PRJEB48885?show=reads>).

## Results

### Clinical isolates collection

We collected a total of 132 samples from 107 patients with difficult-to-treat infections. Difficult-to-treat infections are characterized by conditions that result in poor antibiotic effectiveness, such as biofilms or abscesses, and often require surgical procedures and removal of foreign material in addition to antibiotic treatment

[2,22–24]. To quantify colony growth-delay as a proxy for dormancy depth, we isolated bacteria from these patient samples and plated them on nutrient-rich agar (Fig. 1A). Of the 95 samples yielding growth, 36 samples grew *S. aureus* monocultures (Fig. 1B). They had been recovered from CVIs ( $n = 15$ ; 41.7%), PJIs ( $n = 9$ ; 25.0%), or other clinical categories of infections ( $n = 12$ ; 33.3%; Table S2).

### Patient-derived *S. aureus* exhibit heterogenous colony growth-delays

Colonies resulting from *S. aureus* plated directly after sampling exhibited heterogeneous appearance-times, which led to colony-size heterogeneity (Fig. 1C and D). The degree of appearance-time heterogeneity varied substantially among bacterial populations isolated from different patient samples.

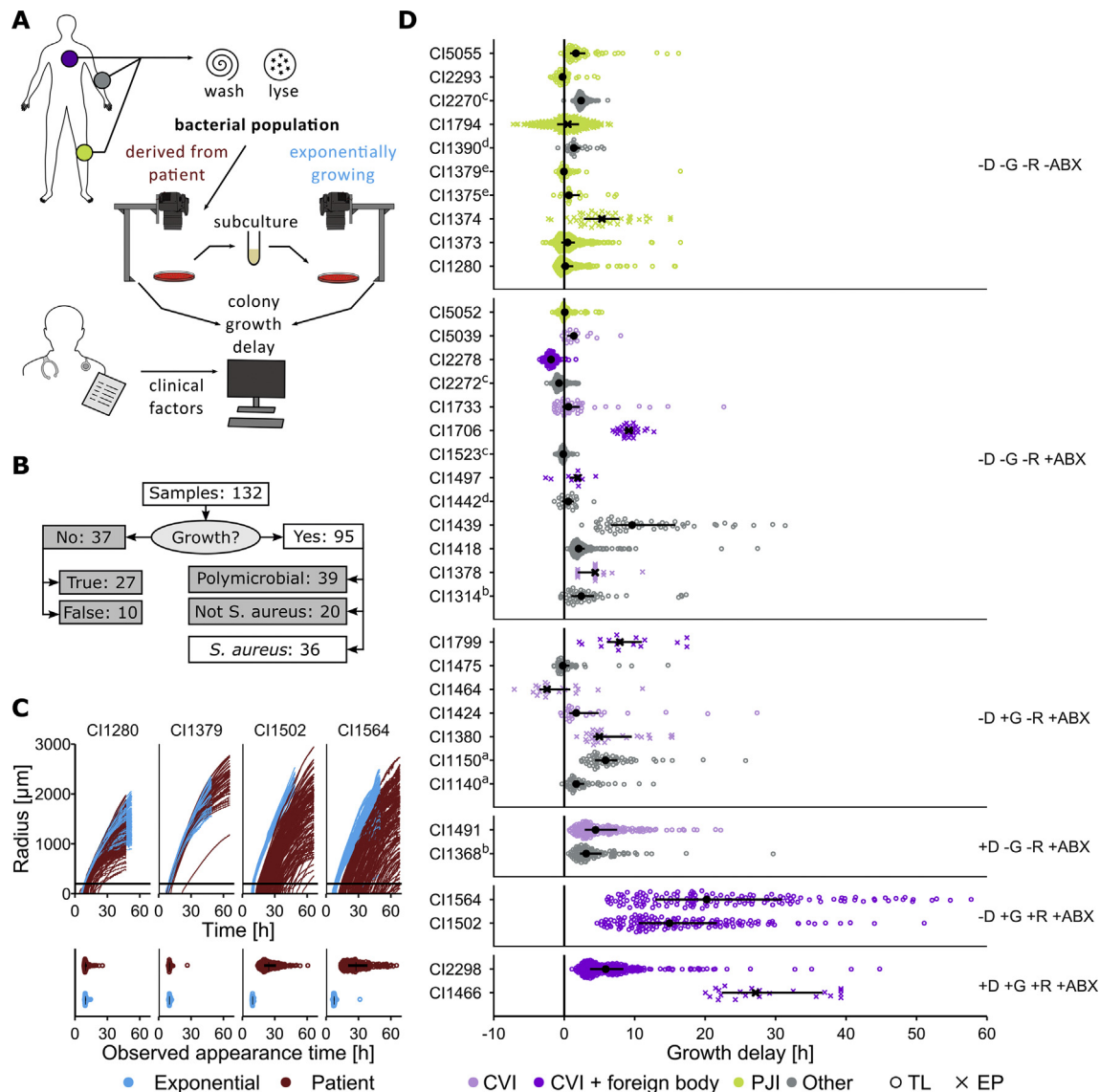


**Fig. 1.** Colony growth-delays of patient-derived *S. aureus*. **A.** Schematic representation of patient sample processing. **B.** Flow-chart representing the study population selection: only *S. aureus* mono-cultures were retained for further analyses. **C.** Top: radial growth curves of colonies formed by patient-derived or exponential-phase bacterial populations (red and blue respectively) from four selected clinical isolates. The black horizontal line corresponds to the threshold of 200 μm for appearance-time determination (Suppl. Method S4). Bottom: corresponding extracted appearance-time distributions. Each dot represents one colony. Interquartile range (IQR) and median are shown in black. **D.** Growth-delay distributions of the 36 patient-derived *S. aureus*. IQR and median are shown in black. Each dot represents one colony, color reflects the clinical category of the infection (PJI, Prosthetic joint infection; CVI, cardiovascular infection) and symbol shape indicates the imaging method used for appearance-time determination (TL, time-lapse images: 26; EP, Endpoint images: 9). Samples originating from the same patient are marked with matching superscript letters (Suppl. Table S2). Populations are grouped by antibiotic treatment prior to sampling (D, daptomycin; G, gentamicin; R, rifampicin; ABX, any other antibiotic class, including beta-lactams, vancomycin, clarithromycin, metronidazole, ciprofloxacin, levofloxacin, tigecycline or tobramycin. Suppl. Tables S3 and S4).

Subculturing of each clinical isolate in nutrient-rich medium and plating it from the exponential growth phase resulted in a reduction in appearance-time heterogeneity (minimal and maximal values of interquartile range of appearance-time distributions of patient-derived and exponential-phase bacterial populations: 0.5–18 hours and 0.2–2 hours, respectively; Fig. 1C, Fig. S1, and S2). Delays in patient-derived populations from the clinical isolate baseline appearance-time were assumed to reflect the environmentally induced phenotypic state of the bacteria. In some cases, most colonies exhibited marginal growth-delays, suggesting that most bacteria recovered from the infection site were actively dividing within patients (Fig. 1C). In other cases, extended growth-delays of up to 57.6 hours were observed, indicating dormant states within patients.

Extreme growth-delays co-occurred with the highest variance (Fig. 1D) and were accompanied by a global increase in delay for the entire population. Previously, we summarized colony growth-delay distributions by quantifying their tail, with an absolute threshold based on radius or appearance-time [12,15,25]. Here, given the correlation of the median of the distributions with the proportion of colonies appearing later than 6 hours (Fig. S7), we used median growth-delay as an estimator of population-wide dormancy.

#### Growth-delay of patient-derived *S. aureus* is associated with antibiotic treatment regimens

To explore which clinical parameters explained patient-derived *S. aureus* median growth-delay, we used a combination of univariable and multivariable linear regression. We included patient and infection characteristics, as well as characteristics of the

within-patient environment encountered by bacteria, including antibiotic treatment of the patient any time prior to sampling, as predictors (Tables S3 and S4).

Clinical category of infection and specific antibiotic treatments were significantly associated with larger growth-delays in univariable analyses. Upon multivariable adjustment, only RIF treatment was significantly associated with larger median growth-delay (mean: 13.3 hours; 95% CI, 7.13–19.6 hours;  $p < 0.001$ ; Fig. 2).

Some effects might have been masked due to the correlation of certain explanatory variables because of inherent differences across types of infection and associated standard of care (Fig. S8). Nonetheless, direction, effect size, and significance of RIF were robust when subsampling the data, i.e. excluding either PJI samples, multiple samples from the same patient except the latest, or all endpoint-imaged samples; or when additionally adjusting for technical variables, i.e. imaging method and preparation delays (Fig. S9). Moreover, effect size and significance of RIF were robust when considering antibiotic treatment 0 or 1 day prior to sampling (Figs. S10 and S11).

When considering the percentage of colonies with growth-delay >6 hours as an outcome, we obtained comparable effects for RIF (mean: 52.0%; 95% CI, 20.3%–83.8%). Additionally, vancomycin treatment was significantly associated with an increased percentage of colonies with large growth-delays (mean: 31.1%; 95% CI, 7.84%–54.4%; Fig. S12). Finally, a linear mixed-effect model with growth-delay of individual colonies as outcome and clinical isolate identifier as random intercept term (to account for correlation between colonies from the same sample) yielded coherent results (RIF effect on per-colony growth-delay mean: 13.8 hours; 95% CI, 7.42–20.1 hours; Fig. S13).

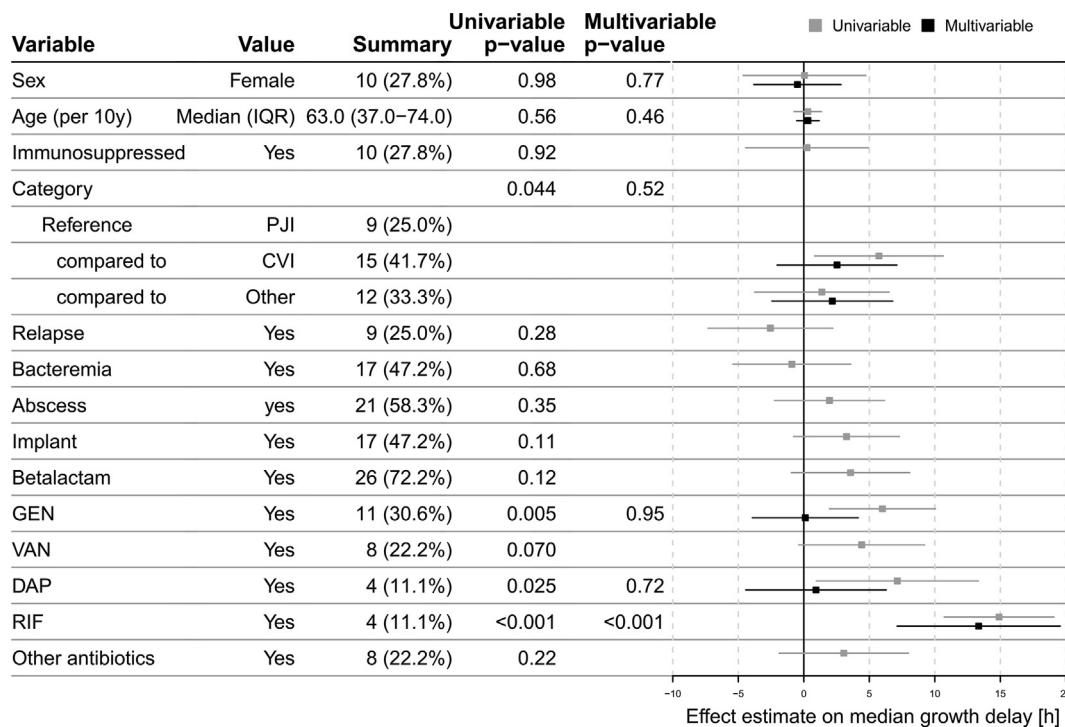


**Fig. 2.** Effect of 14 clinical parameters on the median growth-delay of patient-derived *S. aureus* ( $n = 36$ ), based on univariable and multivariable linear regression. Sex, age, and parameters with a  $p$ -value below 0.05 in the univariable model were included in the multivariable analysis. Categorical and continuous parameters are summarized with count (percentage) for the level indicated or median (interquartile range, IQR), respectively. For the factor clinical category, PJI (prosthetic joint infections) was used as the reference level to which CVI (cardiovascular infections), and other infections were compared to. “Immunosuppressed” indicates that the patient had an immunodeficiency disorder or was under an immunosuppressive treatment. “Relapse” indicates that the infection was considered a relapse from a previous infection based on microbiological and clinical assessment. “Bacteremia” indicates that the patient had one or more positive blood cultures during the course of the infection. “Abscess” (i.e., collection of pus in any section of the body) and “Implant” (i.e., foreign body) indicate the involvement of these clinical entities in the infection. Each antibiotic used to treat the infection was considered. The five antibiotics prescribed to at least four of the 36 patients were included as individual factors. GEN, gentamicin; VAN, vancomycin; DAP, daptomycin; RIF, rifampicin. “Other antibiotics” includes clarithromycin, metronidazole, ciprofloxacin, levofloxacin, tigecycline or tobramycin.

### Biofilm-embedded *S. aureus* surviving high concentrations of rifampicin exhibit increased colony growth-delays

Based on clinical observations, we sought to evaluate the effect of antibiotic exposure on colony growth-delay of *S. aureus* derived from a heterogeneous environment. To mimic this environment *in vitro*, we grew static biofilms with a subset of clinical isolates and exposed them to five routinely used antibiotics with different modes of action at 10× and 100× MIC (Method S7; Table S1).

Bacterial populations derived from biofilms exposed to FLX, clindamycin (CLI), gentamicin (GEN), or levofloxacin (LVX) exhibited colony growth-delay distributions similar to those of the corresponding no-antibiotic control. In contrast, populations derived from biofilms exposed to RIF displayed increased growth-delay (Fig. 3A and Fig. S14). We found that the bacterial load of the biofilm

was not reduced by exposure to most antibiotics, except for the highest LVX concentration and both concentrations of RIF (Fig. 3B).

Overall, our data showed that RIF efficiently killed biofilm-embedded *S. aureus*, but surviving bacteria exhibited an increased delay in growth resumption. However, we did not observe a correlation between median growth-delay and bacterial load according to treatment (Fig. S15).

### Increased growth-delays result in antibiotic tolerance

Next, we investigated whether delays in growth resumption resulting from RIF treatment promote antibiotic tolerance. Therefore, we challenged bacterial populations derived from the biofilm with 40× MIC of the β-lactam FLX in liquid nutrient-rich medium and monitored survival over time. For this experiment, we included four clinical isolates that displayed various levels of growth-delay *ex vivo* (Fig. 1C). Moreover, because RIF is not used as a monotherapy due to the high rate of resistance emergence [26], we additionally included combination treatments of RIF with CLI or LVX.

Any treatment containing RIF reduced the bacterial load significantly (Fig. 4A). The proportion of RIF-resistant mutants in these static cultures was generally low and, as expected, higher with RIF monotherapy ( $0.053\% \pm 0.15\%$ ) than with combination treatments (Fig. 4A; Method S9). With regard to colony growth-delay distributions, any treatment containing RIF resulted in a global shift and longer tail compared with the no-antibiotic control (Fig. 4B and Fig. S16).

When inoculating an equivalent bacterial load from these pre-exposed bacteria in liquid nutrient-rich medium without antibiotics, similar regrowth dynamics were observed. Any treatment containing RIF resulted in prolonged recovery periods of up to 9 hours (Fig. S17). These regrowth kinetics were mirrored by the killing kinetics in the parallel liquid culture that had been supplemented with FLX. Pretreatments, including RIF, resulted in a longer time to kill the same fraction of the population (Fig. 4C) and higher rates of bacterial survival after 24 hours for all but one of the clinical isolates.

In conclusion, exposing *S. aureus* biofilms to RIF monotherapy and combination treatments effectively reduced the viable bacterial load. However, any treatment containing RIF resulted in increased growth-delays, which in three of four tested clinical isolates correlated with increased antibiotic tolerance (Fig. S18).

### Discussion

In this study, we quantified the within-patient occurrence of heterogeneous *S. aureus* growth phenotypes during infections across various clinical presentations. We found that *S. aureus* derived from difficult-to-treat infections commonly exhibit heterogeneity in growth resumption. Yet, we identified substantial differences in the extent of heterogeneity across samples and showed that the widest heterogeneity was associated with RIF treatment.

Our study has several limitations. Notably, unavoidable biases were introduced by the convenience sampling design. Importantly, standard of care for PJIs and CVIs differed substantially: Surgical procedures, from which most samples originated, are part of the reference standard of care for PJIs and more rarely performed to treat CVIs. In our collection, CVIs were severe life-threatening cases treated with antibiotic combinations at the time of surgery. In contrast, most patients with PJIs had not been treated with antibiotics before surgery. Additionally, we considered each antibiotic prescribed as independent explanatory variables, ignoring drug kinetics and dynamics. We speculate that the growth-delay

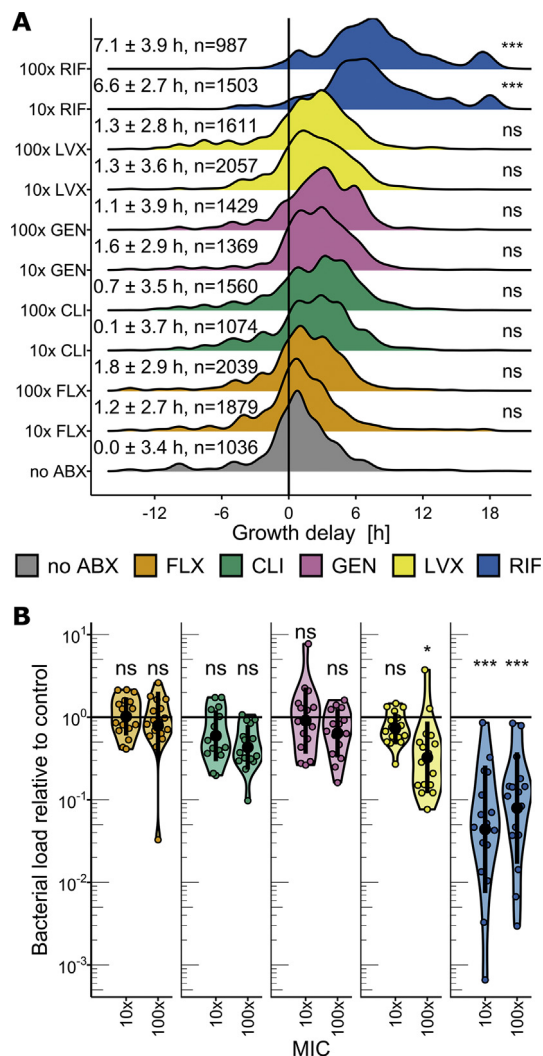


**Fig. 3.** Biofilm assay: screening of 17 clinical isolates. **A.** Growth-delay distributions from biofilm-embedded *S. aureus* populations exposed to either a no-antibiotic control (no ABX) or flucloxacillin (FLX), clindamycin (CLI), gentamicin (GEN), levofloxacin (LVX) or rifampicin (RIF) at 10x and 100x minimum inhibitory concentration (MIC), combining all clinical isolates. Mean and standard deviation of median growth-delay per clinical isolate are shown. n, number colonies included in each distribution. **B.** Biofilm eradication efficacy measured as bacterial load recovered relative to the no-antibiotic control bacterial load. Each dot represents one clinical isolate. Black dots and bars represent mean and standard deviation. ns, non-significant; \*  $p < 0.05$ ; \*\*\*  $p < 0.0001$  based on Dunnett's test comparing all antibiotic and concentration combinations to the no-antibiotic control.

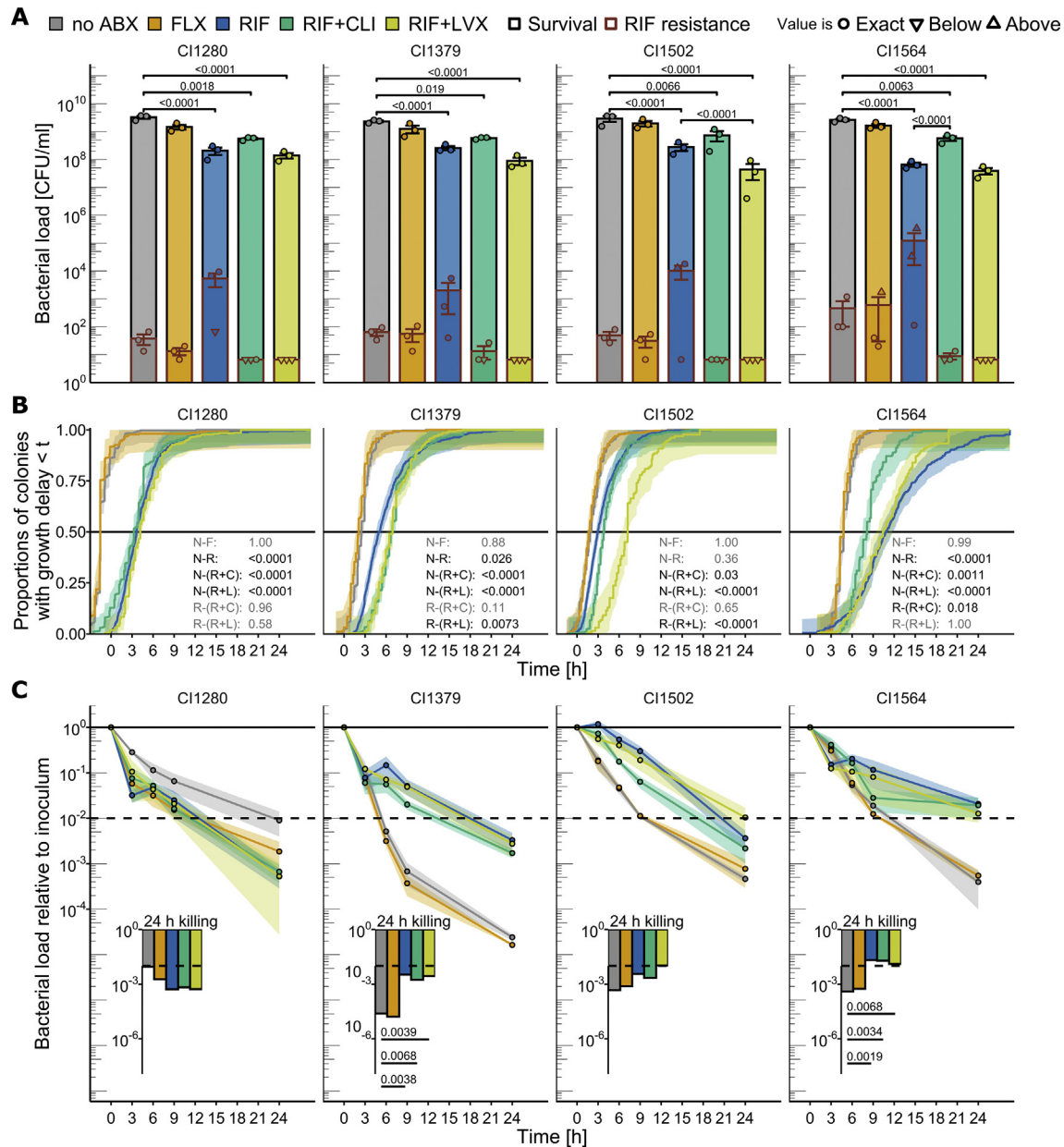


**Fig. 4.** Biofilm assay followed by persistar assay for four clinical isolates **A.** Bacterial load (CFU/ml) of the biofilms for the no-antibiotic control (no ABX) or after exposure to flucloxacillin (FLX), rifampicin (RIF), the combination of rifampicin and clindamycin (RIF+CLI) or rifampicin and levofloxacin (RIF+LVX) (black contour) and corresponding load (CFU/ml) of RIF resistant mutants (overlaid, with a red contour). Mean and standard deviation are shown. Dots represent biological replicates ( $n = 3$ ), and shapes indicate if the value is exact or below/above our detection range (Suppl. Method S7). **B.** Empirical cumulative distribution function of colony growth-delay based on the three biological replicates combined. Shaded area depicts the confidence interval. The black line allows visual extrapolation of median growth-delay for each condition. N, no ABX; F, FLX; R, RIF; R+C, RIF+CLI; R+L, RIF+LVX. All pairwise comparisons performed are indicated and displayed with corresponding p-value in black or grey if significant or non-significant, respectively (e.g., N-F stands for median growth-delay of the no-antibiotic control versus that of the FLX exposed biofilm and is always shown in grey because non-significant). **C.** Time-kill curve upon 40x MIC FLX challenge in liquid medium, with a starting inoculum of approximately  $2 \times 10^5$  CFU/ml achieved by diluting the corresponding static-stationary culture. Dots and shaded area represent mean and standard error of three biological replicates. The dashed line labels a 99% reduction of the initial bacterial load, to allow visual extrapolation of the minimal duration to kill 99% (MDK99). Bacterial load (A), median growth-delay (B) and survival after 24 h 40x MIC FLX challenge (C) were assessed with linear regressions with interaction terms followed by pairwise comparisons computed with estimated marginal means *post-hoc* tests (p-value correction based on multivariate *t*-distribution).

phenotype is likely affected by temporal dynamics and subject to drug interactions instead of the result of additive effects.

Nevertheless, we demonstrated the biological validity of the link between RIF treatment and increased growth-delays with *in vitro* experiments. Concurrently, the performance of RIF in reducing bacterial load was superior to that of other antibiotics, which is consistent with previous studies [24,27]. The co-occurrence of decreased bacterial load and increased median growth-delays

hinders an elucidation of whether RIF treatment induces longer growth-delays or selects a pre-existing subpopulation with long growth-delays by killing the bulk of the population with short growth-delays. Previous literature indicates that antibiotics act as a stressor inducing persistar formation [16,28,29], but our observation of unimodal growth-delay distributions with a higher median and variance upon stress exposure could be explained by selective killing.

Phenotypic heterogeneity in our *in vitro* assays was not driven by genetic heterogeneity (Fig. S6). In our patient cohort, we captured growth phenotypes from single infection sites at one timepoint. However, during long-term infections, within-host genetic diversification may occur and influence stress response [5]. Adding to the temporal dynamics, spatial structure within a host likely influences the phenotypic state of bacteria and could facilitate genetic diversification [4].

In conclusion, by providing an analysis framework and the first epidemiologic description of within-patient *S. aureus* phenotypic heterogeneity, our study lays the groundwork for future studies to dissect complex within-patient bacterial population killing kinetics and evaluate the relevance of the assessment of within-patient bacterial phenotypic heterogeneity for infection prognosis.

### Transparency declaration

### Conflicts of interest

All authors declare no conflict of interests.

### Funding

This work was supported by the University of Zurich, Clinical Research Priority Program “Precision Medicine for Bacterial Infections” (to ASZ and BH), the Swiss National Science Foundation (grant numbers #31003A\_176252 (to ASZ), #320030\_184918/1 (to BH)), and the Promedica Foundation (grant 1449/M (to SDB)).

### Author contributions

SDB, RAS, RDK, BH, and ASZ designed the study. BH and ASZ coordinated the ENVALVE, VASGRA, and BACVIVO cohorts. YA coordinated the PJI cohort. YA, PZ, CAM, SDB, RAS, and ASZ acquired the patient samples. NE, YA, SDB, and BH collected the clinical data. JB, SMS, MH, TAS, and AGM processed the patient samples. JB, MB, SMS, CV, MH, and TAS performed the experiments. JB, MB, SMS, and CV designed and interpreted the experiments. JB, MB, and CV performed the image analysis. JB, MB, and RDK performed the statistical analysis. JB and MB wrote the first draft of the manuscript. SMS, CV, SDB, RDK, BH, and AZ critically revised the manuscript.

### Acknowledgments

We are grateful to our patients for their participation in the study and the study nurses, Caroline Mueller and Simone Buergin, for their excellent work. We also thank Christine Laich and Christine Voegtli for administrative assistance and the technicians of the Institute of Medical Microbiology of the University of Zurich for their expert help and assistance. We thank Vera Beusch and Milos Duknic for assistance with the preliminary data analysis.

### Appendix A. Supplementary data

Supplementary data to this article can be found online at <https://doi.org/10.1016/j.cmi.2022.01.021>.

### References

- [1] Lowy FD. *Staphylococcus aureus* infections. *N Engl J Med* 1998;339:520–32.
- [2] Lebeaux D, Ghigo JM, Beloin C. Biofilm-related infections: bridging the gap between clinical management and fundamental aspects of recalcitrance toward antibiotics. *Microbiol Mol Biol Rev* 2014;78:510–43.
- [3] Foster TJ. Antibiotic resistance in *Staphylococcus aureus*. Current status and future prospects. *FEMS Microbiol Rev* 2017;41:430–49.
- [4] Haunreiter VD, Boumassoud M, Häffner N, Wipfli D, Leimer N, Rachmühl C, et al. In-host evolution of *Staphylococcus epidermidis* in a pacemaker-associated endocarditis resulting in increased antibiotic tolerance. *Nat Commun* 2019;10:1149.
- [5] Liu J, Gefen O, Ronin I, Bar-Meir M, Balaban NQ. Effect of tolerance on the evolution of antibiotic resistance under drug combinations. *Science* 2007;317:200–204.
- [6] Balaban NQ, Helaine S, Lewis K, Ackermann M, Aldridge B, Andersson DI, et al. Definitions and guidelines for research on antibiotic persistence. *Nat Rev Microbiol* 2019;17:441–8.
- [7] Huemer M, Mairpady Shambat S, Brugger SD, Zinkernagel AS. Antibiotic resistance and persistence—Implications for human health and treatment perspectives. *EMBO Rep* 2020;21:e51034.
- [8] Brauner A, Fridman O, Gefen O, Balaban NQ. Distinguishing between resistance, tolerance and persistence to antibiotic treatment. *Nat Rev Microbiol* 2016;14:320–30.
- [9] Proctor RA, Eiff C von, Kahl BC, Becker K, McNamara P, Herrmann M, et al. Small colony variants: a pathogenic form of bacteria that facilitates persistent and recurrent infections. *Nat Rev Microbiol* 2006;4:295–305.
- [10] Tuchscherl L, Medina E, Hussain M, Völker W, Heitmann V, Niemann S, et al. *Staphylococcus aureus* phenotype switching: an effective bacterial strategy to escape host immune response and establish a chronic infection. *EMBO Mol Med* 2011;3:129–41.
- [11] Conlon BP. *Staphylococcus aureus* chronic and relapsing infections: evidence of a role for persister cells: an investigation of persister cells, their formation and their role in *S. aureus* disease. *BioEssays News Rev Mol Cell Dev Biol* 2014;36:991–6.
- [12] Huemer M, Shambat SM, Bergada-Pijuan J, Söderholm S, Boumassoud M, Vulin C, et al. Molecular reprogramming and phenotype switching in *Staphylococcus aureus* lead to high antibiotic persistence and affect therapy success. *Proc Natl Acad Sci U S A* 2021;118:e2014920118.
- [13] von Eiff C, Peters G, Becker K. The small colony variant (SCV) concept—the role of staphylococcal SCVs in persistent infections. *Injury* 2006;37:S26–33.
- [14] de Souza DC, Cogo LL, Palmeiro JK, Dalla-Costa LM, de Oliveira Tomaz AP, Riedi CA, et al. Thymidine-auxotrophic *Staphylococcus aureus* small-colony variant bacteremia in a patient with cystic fibrosis. *Pediatr Pulmonol* 2020;55:1388–93.
- [15] Vulin C, Leimer N, Huemer M, Ackermann M, Zinkernagel AS. Prolonged bacterial lag time results in small colony variants that represent a sub-population of persisters. *Nat Commun* 2018;9:4074.
- [16] Johnson PJT, Levin BR. Pharmacodynamics, population dynamics, and the evolution of persistence in *Staphylococcus aureus*. *PLoS Genet* 2013;9:e1003123.
- [17] Lewis K. Persister cells and the riddle of biofilm survival. *Biochem Biophys Res Commun* 2005;330:267–74.
- [18] Barr DA, Kamdolozi M, Nishihara Y, Ndhlovu V, Khonga M, Davies GR, et al. Serial image analysis of Mycobacterium tuberculosis colony growth reveals a persistent subpopulation in sputum during treatment of pulmonary TB. *Tuberc Edinb Scotl* 2016;98:110–5.
- [19] Bär J, Boumassoud M, Kouyos RD, Zinkernagel AS, Vulin C. Efficient microbial colony growth dynamics quantification with ColTapp, an automated image analysis application. *Sci Rep* 2020;10:16084.
- [20] Wickham H. ggplot2: elegant graphics for data analysis. Available at: <https://ggplot2.tidyverse.org>. [Accessed 28 June 2021].
- [21] Lenth RV, Buerkner P, Herve M, Love J, Riebl H, Singmann H. emmeans: estimated marginal means, aka least-squares means. Available at: <https://CRAN.R-project.org/package=emmeans>. [Accessed 28 June 2021].
- [22] de Marie S. Difficult-to-treat infections. *Intensive Care Med* 1990;16:S239–42.
- [23] Chakfé N, Diener H, Lejay A, Assadian O, Berard X, Caillon J, et al. Editor's choice - European society for vascular surgery (ESVS) 2020 clinical practice guidelines on the management of vascular Graft and endograft infections. *Eur J Vasc Endovasc Surg* 2020;59:339–84.
- [24] Zimmerli W, Sendi P. Role of rifampin against *Staphylococcal* biofilm infections *in vitro*, in animal models, and in orthopedic-device-related infections. *Antimicrob Agents Chemother* 2019;63:e01746–18.
- [25] Häffner N, Bär J, Dengler Haunreiter V, Mairpady Shambat S, Seidl K, Crosby HA, et al. Intracellular environment and *agr* system affect colony size heterogeneity of *Staphylococcus aureus*. *Front Microbiol* 2020;11:1415.
- [26] Russell CD, Lawson McLean A, Saunders C, Laurenson IF. Adjunctive rifampicin may improve outcomes in *Staphylococcus aureus* bacteraemia: a systematic review. *J Med Microbiol* 2014;63:841–8.
- [27] Jørgensen NP, Skovdal SM, Meyer RL, Dagnæs-Hansen F, Fuursted K, Petersen E. Rifampicin-containing combinations are superior to combinations of vancomycin, linezolid and daptomycin against *Staphylococcus aureus* biofilm infection *in vivo* and *in vitro*. *Pathog Dis* 2016;74:ftw019.
- [28] Kwan BW, Valenta JA, Benedik MJ, Wood TK. Arrested protein synthesis increases persister-like cell formation. *Antimicrob Agents Chemother* 2013;57:1468–73.
- [29] Dörr T, Lewis K, Vulić M. SOS response induces persistence to fluoroquinolones in *Escherichia coli*. *PLoS Genet* 2009;5:e1000760.